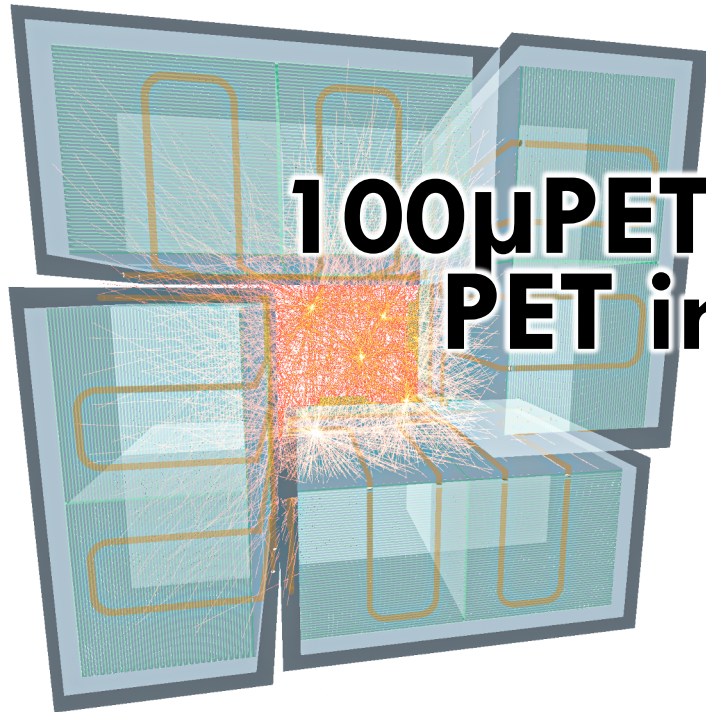




UNIVERSITÉ  
DE GENÈVE



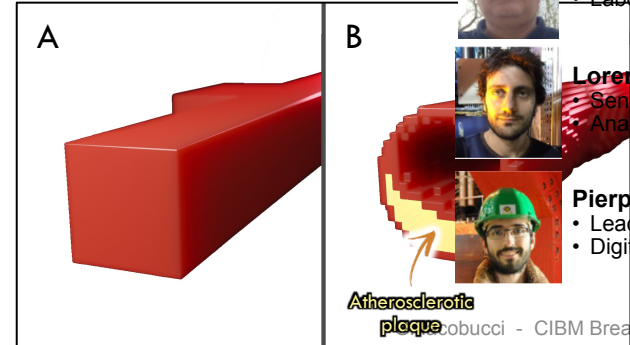
# 100 $\mu$ PET: Ultra-high-resolution PET imaging with MAPS

18th Trento workshop  
28 Feb - 2 Mar 2023

Mateus Vicente  
on behalf of the 100 $\mu$ PET collaborators

# Introduction

- The **100 $\mu$ PET** project: molecular imaging with ultra-high resolution
  - **SNSF SINERGIA** grant among **UNIGE** (scanner production) **EPFL** (imaging) and **UNILU** (medical application studying atherosclerosis in ApoE<sup>+/−</sup> mice)
    - Deliverable: Small-animal PET scanner with monolithic silicon pixel detectors
- Talk outline
  - Introduction to PET and spatial resolution overview
  - How ultra-high resolution is aimed
  - The 100 $\mu$ PET scanner
    - Flip-chip prototyping and reliability tests
    - Monte-Carlo performance simulations
    - Imaging capabilities
  - Summary and Conclusions



Images: © Xavier Ravinet - UNIGE

With today's PET technology, small blood vessels can only be visualized in their entirety (A). The proposed new PET technology will allow the study of changes in the walls of small blood vessels, such as atherosclerotic plaques (B).

## The 100 $\mu$ PET project



**Giuseppe Iacobucci**  
 • project P.I.  
 • System design



**Yannick Favre**  
 • Board design  
 • RO system



**Roberto Cardella**  
 • Sensor design  
 • Laboratory test



**Lorenzo Paolozzi**  
 • Sensor design  
 • Analog electronics



**Stéphane Débieux**  
 • Board design  
 • RO system



**Mateus Vicente**  
 • System integration  
 • Laboratory test



**Didier Ferrere**  
 • System integration  
 • Laboratory test



**Franck Cadoux**  
 • Mechanical design



**Jihad Saidi**  
 • Detector simulation  
 • Data analysis



**Sergio Gonzalez-Sevilla**  
 • System integration  
 • Laboratory test



**Thanushan Kugathasan**  
 • Lead chip design  
 • Digital electronics



**Luca Iodice**  
 • Chip design  
 • Firmware



**Martin Walter**  
 • P.I.



**Pablo Jané**  
 • Nuclear Medicine  
 • PET imaging  
 • Translational imaging



**Vincent Taelman**  
 • Molecular biology  
 • Radiopharmacy



**Michaël Unser**  
 • P.I.



**Pol del Aguila Pla**  
 • Statistical signal processing



**Aleix Boquet-Pujadas**  
 • Signal/image processing  
 • Physical modeling



**Antonio Picardi**  
 • Chip design  
 • Firmware



**Stefano Zambito**  
 • Laboratory test  
 • Data analysis



**Matteo Milanesio**  
 • Laboratory test  
 • Data analysis



**Théo Moretti**  
 • Laboratory test  
 • Data analysis



**Carlo A. Fenoglio**  
 • Chip design  
 • Firmware



**Chiara Magliocca**  
 • Laboratory test  
 • Data analysis



**Jordi Sabater**  
 • Detector simulation  
 • Laboratory test



**Rafaella Kotitsa**  
 • Sensor simulation



UNIVERSITÉ  
DE GENÈVE

UNIVERSITY OF  
LUCERNE

EPFL

### Main research partners:



**Roberto Cardarelli**  
 INFN Rome2 & UNIGE



**Holger Rücker**  
 IHP Mikroelektronik



**Marzio Nesi**  
 CERN & UNIGE



**Matteo Elviretti**  
 IHP Mikroelektronik

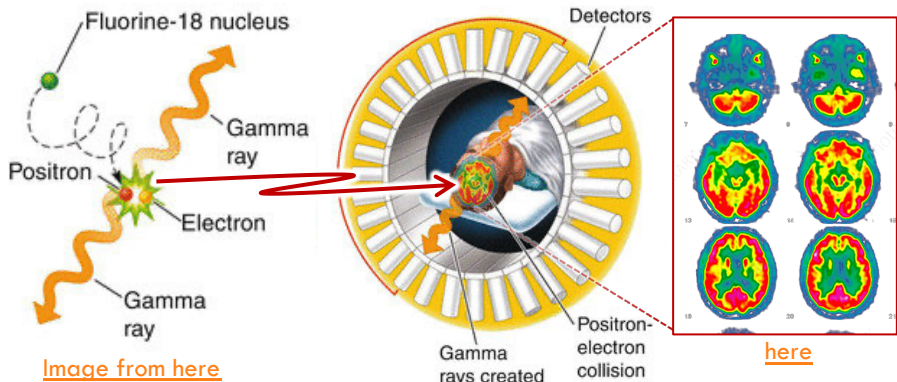
### Funded by:



# Positron Emission Tomography (PET)

4

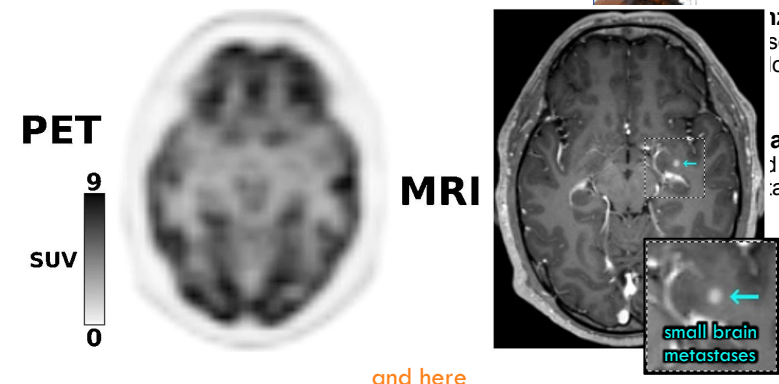
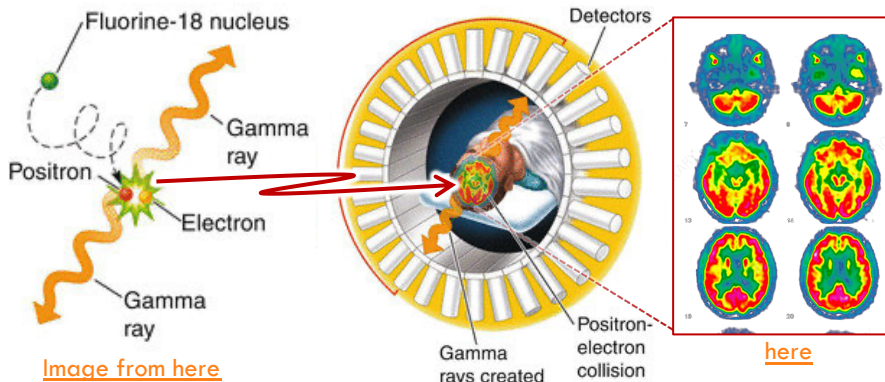
- PET is a nuclear medicine method to study metabolic processes in the body
  - Radiotracer is injected in a body; Positrons from the radionuclide annihilates with electrons of the nearby tissue
    - Two back-to-back 511 KeV photons are emitted and detected in coincidence
      - Lines-of-Response (LoR) are defined by the volume between the sensitive elements detecting the two photons
  - Lines-of-response are processed to generate density maps of the detected annihilations



# Positron Emission Tomography (PET)

5

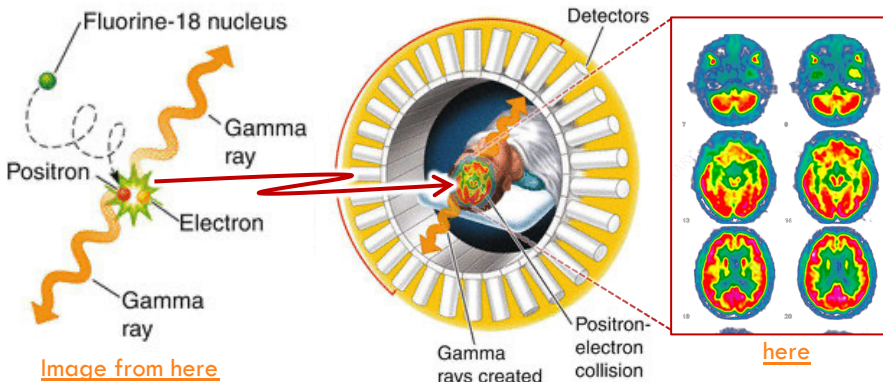
- PET is a nuclear medicine method to study metabolic processes in the body
  - Radiotracer is injected in a body; Positrons from the radionuclide annihilates with electrons of the nearby tissue
    - Two back-to-back 511 KeV photons are emitted and detected in coincidence
      - Lines-of-Response (LoR) are defined by the volume between the sensitive elements detecting the two photons
  - Lines-of-response are processed to generate density maps of the detected annihilations
    - Today, due to the lack of spatial resolution, PET imaging must be done in hybrid mode (combining MRI or CT measurements)



# Positron Emission Tomography (PET)

6

- PET is a nuclear medicine method to study metabolic processes in the body
  - Radiotracer is injected in a body; Positrons from the radionuclide annihilates with electrons of the nearby tissue
  - Two back-to-back 511 KeV photons are emitted and detected in coincidence
    - Lines-of-Response (LoR) are defined by the volume between the sensitive elements detecting the two photons
  - Lines-of-response are processed to generate density maps of the detected annihilations
    - Today, due to the lack of spatial resolution, PET imaging must be done in hybrid mode (combining MRI or CT measurements)
      - Typical resolution is in the range of **1-2 mm<sup>3</sup>**

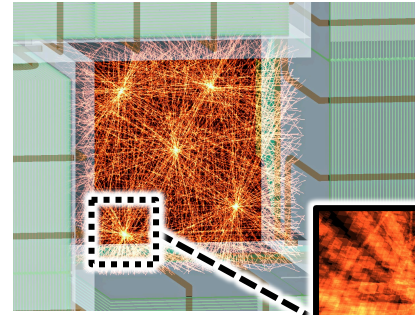
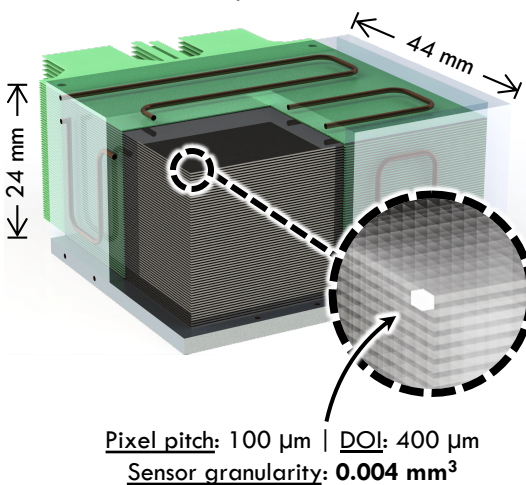


# PET imaging using MAPS

7

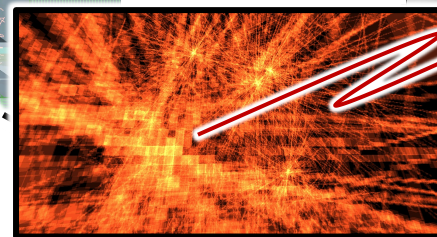
- Ultra-high resolution can be achieved increasing the detection volume granularity,
  - ▣ Multi-layers of monolithic pixel detectors, reducing the volume-of-response by **80'000** (w.r.t.  $4 \times 4 \times 20 \text{ mm}^3$  scintillators)
    - Allowing fast LoR 3D histogramming for online monitoring, without standard PET reconstruction, for example

Render of 60 layers of MAPS stacked

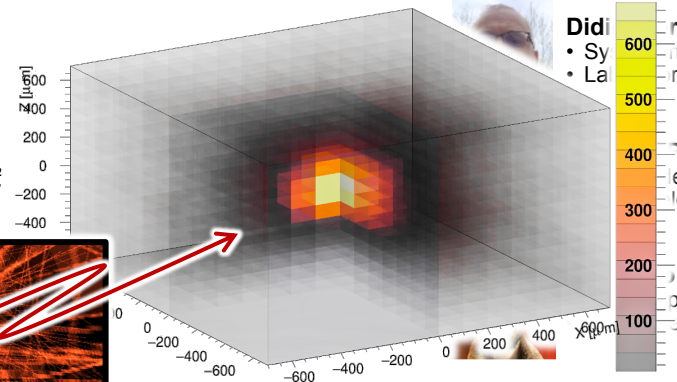


Superposition of all LoR reconstructed from 5 point sources measured with the 100 $\mu$ PET scanner

Voxels of  
100 x 100 x 100  $\mu\text{m}^3$



3D histogram centered at a given source position, counting LoR at each space



# Limit in spatial resolution in PET imaging

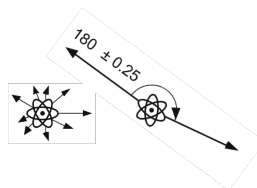
8

- How good can PET spatial resolution be?  
What are the limitations to pinpoint the positron source?

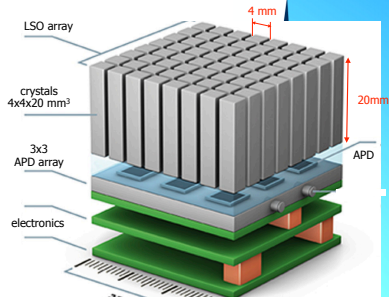
## Fundamental

**Positron range:**  $102\mu\text{m}$  FWHM for F18

**Acolinearity:**  $90\mu\text{m} \approx 4 \cdot 10^{-3}R$

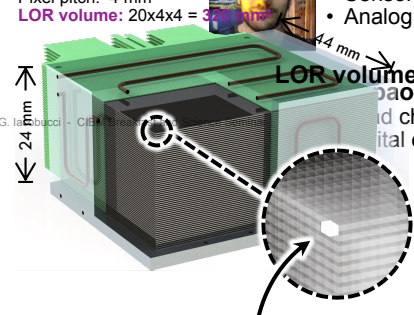


detector = detection channel pitch  
 $o$  = Offset from the center  
 $h$  = Depth-of-interaction  
 $R$  = Radius of the FOV



Conventional PET scanner module

Crystal pitch: 4000  $\mu\text{m}$  | DOI: 20000  $\mu\text{m}$



100 $\mu$ PET detection tower

Pixel pitch: 100  $\mu\text{m}$  | DOI: 400  $\mu\text{m}$

# The 100 $\mu$ PET

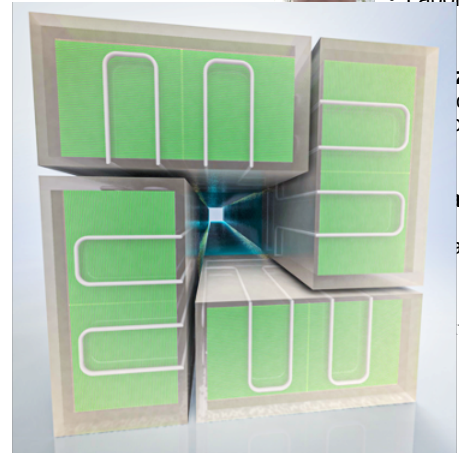
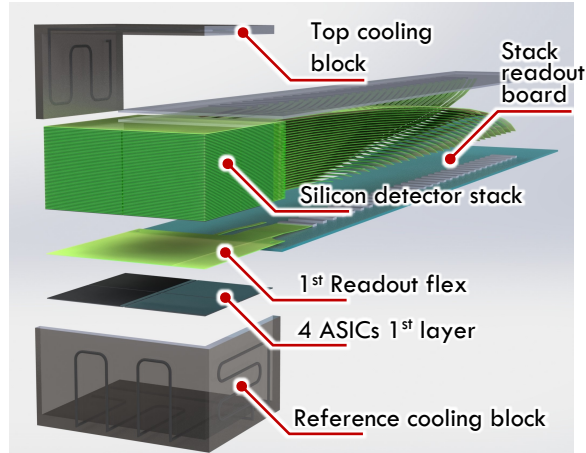
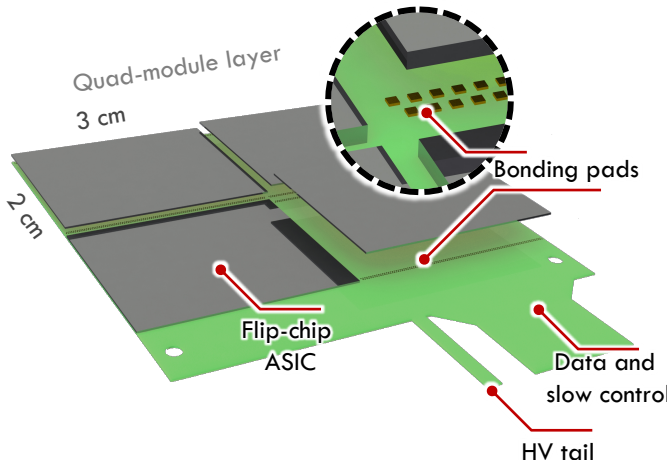
## ASIC, module/layer, tower and scanner

9

myicente@cern.ch

- Multi-layer stack of CMOS imaging sensors based on silicon pixel detectors used in HEP
  - Monolithic 100 $\mu$ PET ASIC: 130 nm SiGe BiCMOS\*; **2.2 x 3 cm<sup>2</sup>**; 100  $\mu$ m pixel pitch; 270  $\mu$ m thick; ~1W power
  - Single silicon detection layer composed by **2x2 ASICs flip-chip** to a flex printed circuit, covering ~30 cm<sup>2</sup>
    - Optional 50  $\mu$ m thick **Bismuth** layer to increase the photon conversion efficiency (w.r.t. only silicon)
  - **60** detection layers compose each scanner **tower**, with 4 towers per scanner (for a grand total of **960 chips!**)

\*check talks from  
Stefano Z. and Matteo M.

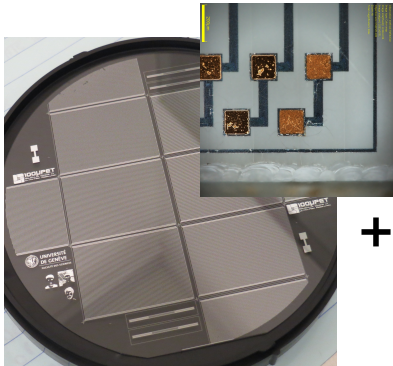


# Module assembly

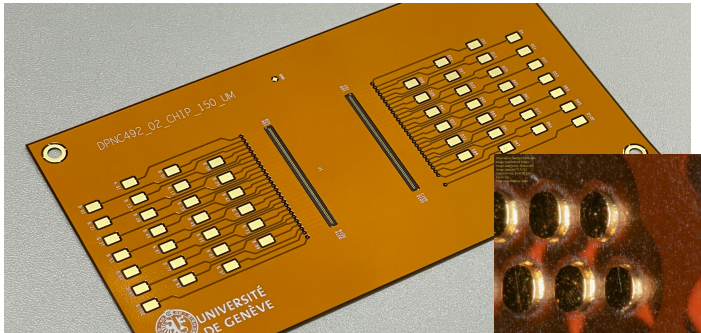
## Flip-chip bonding with a pad-wafer

10

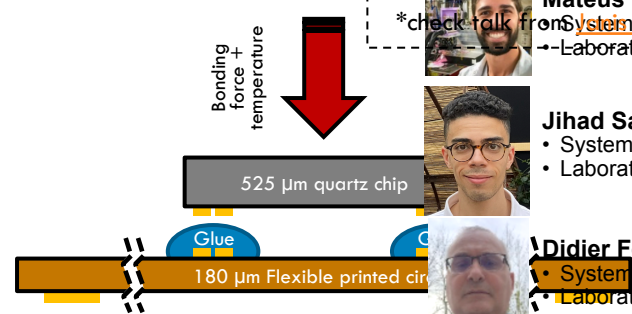
- Pad-wafer produced at CMi (EPFL) with flip-chip pad-chain structure
  - 525 µm thick. Single layer Ti/Al metal patterning + ENIG plating (CERN)
- Flex designed to measure flip-chip bonding yield
  - 4 layers, ~180 µm total thickness. ENIG pad finishing
- Chip's IO pad design driven by chosen (standard) FPC technology
  - Pads 125 µm wide, 250 µm pitch, 2 rows (**238 IO pads** over one 30 mm edge)



+

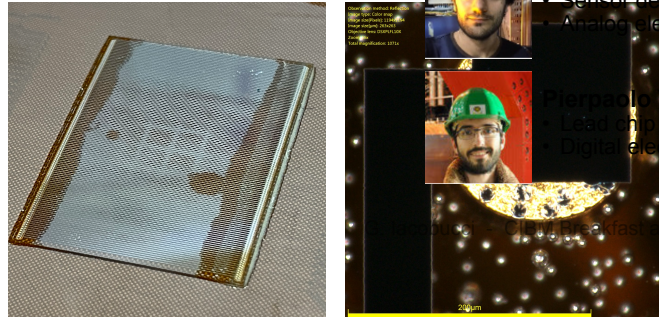


Pad wafer with 6 full chain dies



myicente@cern.ch

\*check talk from [Janis S.](#)



Prototyping flex

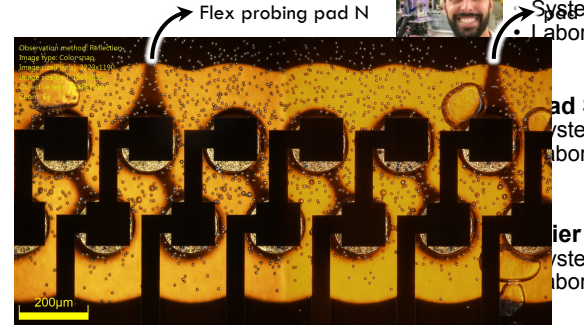
Flip-chip bonded test assembly

# Module assembly

## First reliability tests

11

- 2-wire measurements of the full chain, or individual segments with 8 pads
  - Quantitative measurement limited to check open or closed connection
    - Bonding tool smaller than test chip → Lower bonding force in chip edges
- Reliability tests with up to 100 temperature cycles from +5 to +60 °C



Chain segment with 8 pads connection

3 Samples in the climate chamber



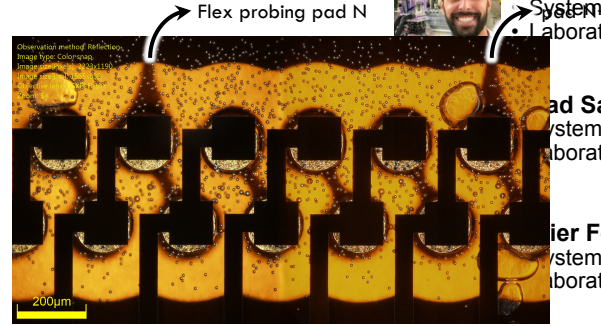
# Module assembly

## First reliability tests

12

mvicente@cern.ch

- 2-wire measurements of the full chain, or individual segments with 8 pads
  - Quantitative measurement limited to check open or closed connection
    - Bonding tool smaller than test chip → Lower bonding force in chip edges
- Reliability tests with up to 100 temperature cycles from +5 to +60 °C
  - Very promising results with first samples produced...



Chain segment with 8 pads connection

3 Samples in the climate chamber



Resistance measurements for top and bottom edges (systematic flex/probing resistance not corrected)

	Top edge [#chain segment]														Bottom edge [#chain segment]																																	
	5	6	7	8	9	10	11	12	13	14	15	16	17	18	19	20	21	22	23	24	25	26	27	5	6	7	8	9	10	11	12	13	14	15	16	17	18	19	20	21	22	23	24	25	26	27		
Initial	2.3	2.4	2.2	2.2	2.2			2.1	2.2	2.2	2.1	1.8	2	2.1	1.9	1.8	1.9	2	2	1.8	2.1	2	2.2		2.4	2.4	2.4	4.5	2.4	2.2	1.9	1.8	2	2.1	2	1.9	2	2.1	2	2.3	2.2	2.2	1.9	1.9	2.3	2.4		
After 40°C	2.2	2.2	2.2	2.2	2.2			1.9	2.3	2.2	2.1	1.8	2	2.1	2	1.9	1.9	2.1	2.1	1.9	2.1	2.2	2.3		2.4	2.4	2.5	6.1	2.5	2.3	2	1.8	2	2.1	2	1.9	2.1	2	2.2	2	3.3	2.1	2.1	1.9	2	2.3	2.5	
1 cycle	2.4	2.5	2.4	2.4	2.4			2.2	2.5	2.4	2.2	2	2.2	2.4	2.2	1.9	2	2.2	2.2	2	2.2	2.3	2.4		7.4	7.4	7.5	10.4	7.6	7.4	7.5	2.4	2.6	2.7	2.6	2.5	2.6	2.7	2.5	2.5	2.6	3.2	2.9	2.9	3.1	3	3.3	3.4
3 cycles	2.5	2.5	2.5	2.4	2.4			2.1	2.7	2.3	2.2	2	2.2	2.2	2.1	2.1	2.3	2.2	2.1	2.3	2.4	2.5		2.6	2.6	2.8	6.6	2.9	2.5	2.2	2	2.2	2.3	2.2	2.1	2.1	2.2	2.1	2.1	2.5	2.5	2.6	2.3	2.3	2.7	2.7		
5 cycles	2.6	2.5	2.5	2.4	2.4			2.1	2.7	2.3	2.3	2	2.2	2.3	2.2	2.1	2.1	2.3	2.2	2.1	2.3	2.4	2.5		2.7	2.6	2.8	6.5	2.9	2.5	2.2	2	2.2	2.3	2.2	2.1	2.1	2.4	2.3	2.3	2	2.1	2.1	2.6				
11 cycles	19.3	2.4	2.3	2.3	2.2			2	1.9	2.1	2.2	2	1.9	2	2.2	2.1	2	2.2	2.3	2.4	2.7	2.5	2.6	5.8	2.7	2.4	2.1	1.9	2.1	2.2	2.1	1.9	2	2.3	2	2.1	2.4	2.2	2.3	2	2	2.4	4.2					
35 cycles			21.2	2.3	2.2			2	2.6	2.2	2.1	1.9	2.1	2.2	2	1.9	2	2.2	2.1	2	2.2	2.3	2.4		2.7	2.7	2.8	4.9	2.7	2.4	2.1	1.9	2.1	2.2	2.1	1.9	2	2.1	2	2	2.3	2.3	2	2	2.5	17.4		

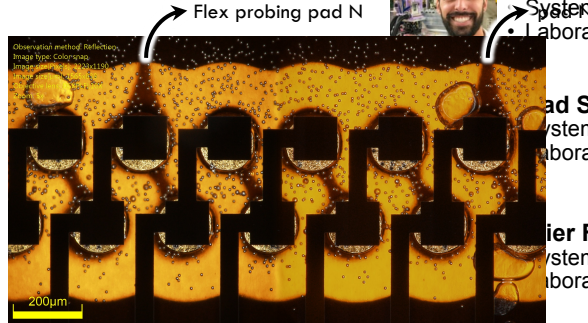
# Module assembly

## First reliability tests

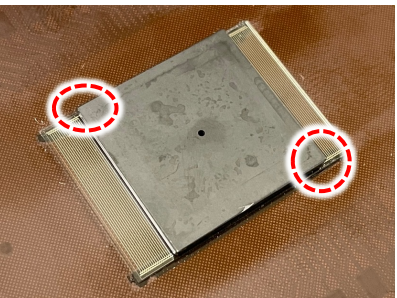
13

mvicente@cern.ch

- 2-wire measurements of the full chain, or individual segments with 8 pads
  - Quantitative measurement limited to check open or closed connection
    - Bonding tool smaller than test chip → Lower bonding force in chip edges
- Reliability tests with up to 100 temperature cycles from +5 to +60 °C
  - Very promising results with first samples produced...
    - On-going tests with new samples implementing new bonding features
      - e.g.: Larger glue underfill for mechanical reinforcement at the extreme edges



Sample with SiC bonding tool on top



Resistance measurements for top and bottom edges (systematic flex/probing resistance not corrected)

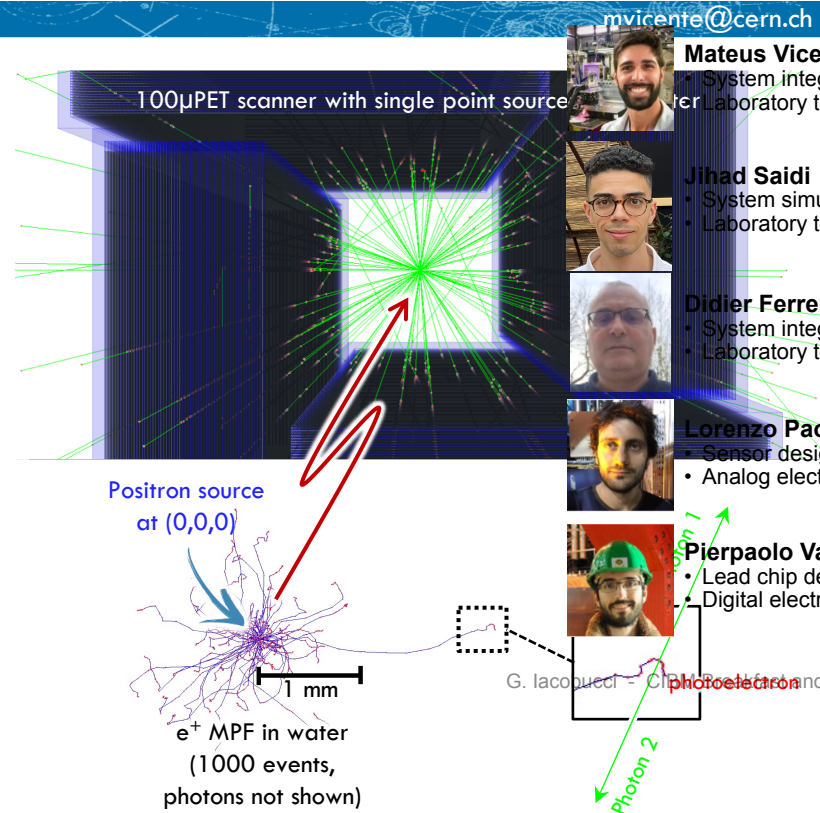
	Top edge [#chain segment]																												Bottom edge [#chain segment]																										
	5	6	7	8	9	10	11	12	13	14	15	16	17	18	19	20	21	22	23	24	25	26	27	5	6	7	8	9	10	11	12	13	14	15	16	17	18	19	20	21	22	23	24	25	26	27									
Initial	2,3	2,4	2,2	2,2	2,2			2,1	2,2	2,2	2,1	1,8	2	2,1	1,9	1,8	1,9	2	2	1,8	2,1	2	2,2		2,4	2,4	2,4	4,5	2,4	2,2	1,9	1,8	2	2,1	2	1,9	2	2,1	2	2,3	2,2	2,2	1,9	1,9	2,3	2,4									
After 40°C	2,2	2,2	2,2	2,2	2,2			1,9	2,3	2,2	2,1	1,8	2	2,1	2	1,9	1,9	2,1	2,1	1,9	2,1	2,2	2,3		2,4	2,4	2,5	6,1	2,5	2,3	2	1,8	2	2,1	2	1,9	2,1	2	2	2	3,3	2,1	2,1	1,9	2	2,3	2,5								
1 cycle	2,4	2,5	2,4	2,4	2,4			2,2	2,5	2,4	2,2	2	2,2	2,4	2,2	1,9	2	2	2,2	2,2	2	2,2	2,3	2,4		7,4	7,4	7,5	10,4	7,6	7,4	7,5	2,4	2,6	2,7	2,6	2,5	2,6	2,7	2,5	2,5	2,6	3,2	2,9	2,9	3,1	3	3,3	3,4						
3 cycles	2,5	2,5	2,5	2,5	2,4	2,4		2,1	2,7	2,3	2,2	2	2,2	2,2	2,1	2,1	2,3	2,2	2,1	2,3	2,4	2,5		2,6	2,6	2,8	6,6	2,9	2,5	2,2	2	2,2	2,3	2,2	2,1	2,1	2,2	2,1	2,1	2,5	2,5	2,6	2,3	2,3	2,7	2,7									
5 cycles								2,1	2,7	2,3	2,3	2	2,2	2,3	2,2	2,2	2,1	2,1	2,3	2,2	2,1	2,3	2,4		2,7	2,6	2,8	6,5	2,9	2,5	2,2	2	2,2	2,3	2,2	2,1	2,1	2,4	2,3	2,3	2	2,1	2,1	2,6											
11 cycl								2,4	2,4																2,7	2,5	2,6	5,8	2,7	2,4	2,1	1,9	2,1	2,2	2,1	1,9	2	2,3	2	2,1	2,4	2,2	2,3	2	2	2	4,2								
35 cycl								19,3	2,4	2,3	2	2,2													2,2	2,6	2,2	2,1	1,9	2,1	2,2	2,1	1,9	2,1	2,2	2,1	1,9	2	2,1	2	2,3	2,3	2	2	2	17,4									
								21,2																	2	2,6	2,2	2,1	1,9	2,1	2,2	2,1	1,9	2,1	2,2	2,1	1,9	2	2,1	2	2,3	2,3	2	2	2										

NB: Start of disconnection at the far edges where the maximum stress is concentrated

# Performance simulations

14

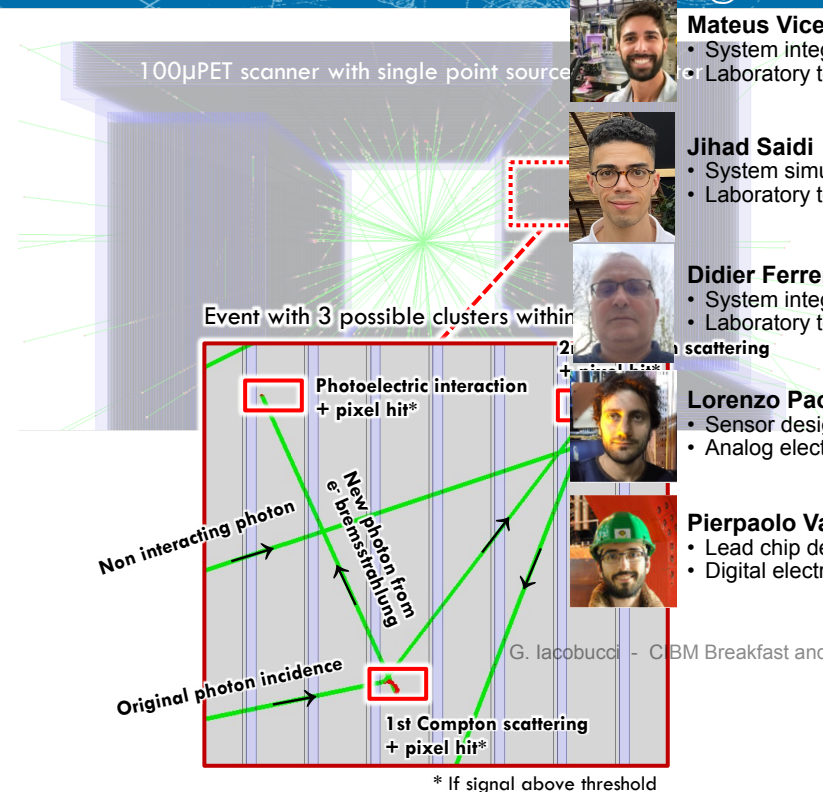
- Full Monte Carlo (Geant4 + AllPix<sup>2</sup>) simulations
  - Full scanner geometry (w/ or w/o Bi layers) + water volume
  - Positron mean free path and annihilation from  $[^{18}\text{F}]$ FDG
  - Photon interactions (scattering and photoelectric effect)
  - Sensor/ASIC response + pixel clustering
- Single positron annihilation per event (no time information)
  - Event filtering for **unambiguous** line-of-response acceptance
    - Only events with two scanner towers having each a single cluster
  - No energy window for discriminating signals from Compton or photoelectric interactions
- Positron sources:
  - Single point; Derenzo phantom; High resolution medical images



# Performance simulations

15

- **Full Monte Carlo (Geant4 + AllPix<sup>2</sup>) simulations**
  - Full scanner geometry (w/ or w/o Bi layers) + water volume
  - Positron mean free path and annihilation from [<sup>18</sup>F]FDG
  - Photon interactions (scattering and photoelectric effect)
  - Sensor/ASIC response + pixel clustering
- Single positron annihilation per event (no time information)
  - Event filtering for **unambiguous** line-of-response acceptance
    - Only events with two scanner towers having each a single cluster
  - No energy window for discriminating signals from Compton or photoelectric interactions
- Positron sources:
  - Single point; Derenzo phantom; High resolution medical images

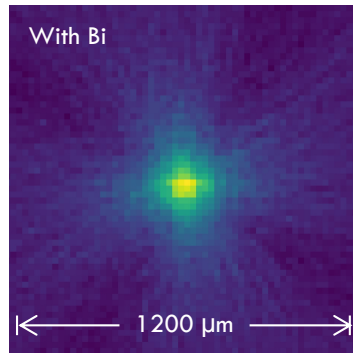
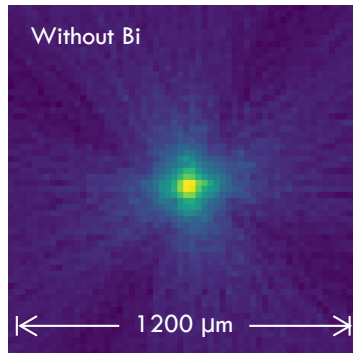


# Performance simulations

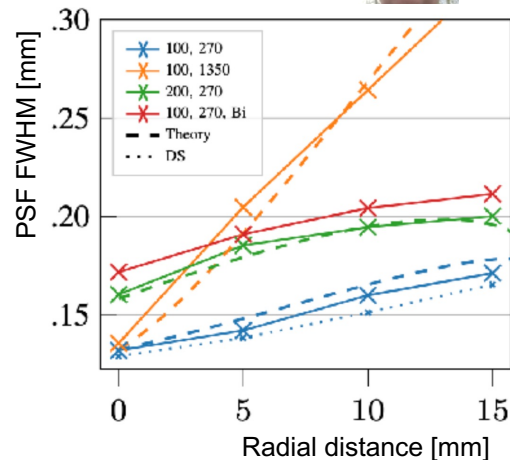
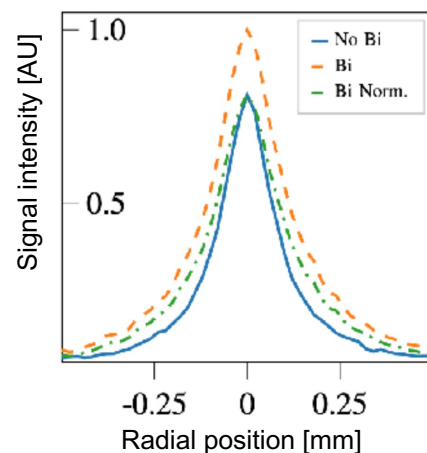
## Single point source: Sensitivity and resolution

16

- **Sensitivity:** amount of unambiguous LoR measured as a function of the total number of positrons
  - 3.3% and 4.8% detection efficiency, with and without Bi respectively
- **Spatial resolution:** Point Spread Function with FBP (Filtered Back Projection)
  - 0.13 mm, lowered to 0.17 with Bi absorber layer ( $\pm 0.014$  mm)
- ➡ Very small parallax distortion! Investigating effect of 50  $\mu$ m Bi with 200  $\mu$ m pixel pitch
  - Higher sensitivity; slight lower spatial resolution; 1/4<sup>th</sup> of the number of channels (lower power!)



Reconstructed point source  
Bin size: 20  $\mu$ m

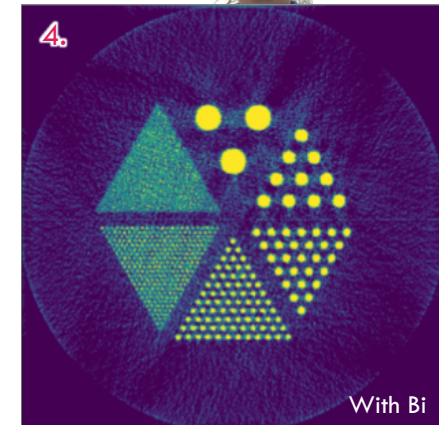
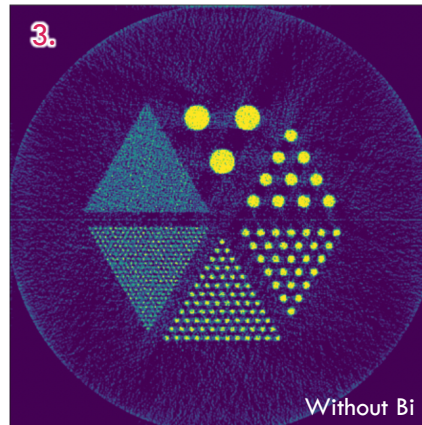
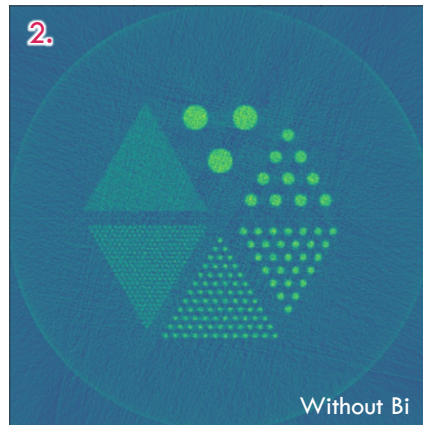
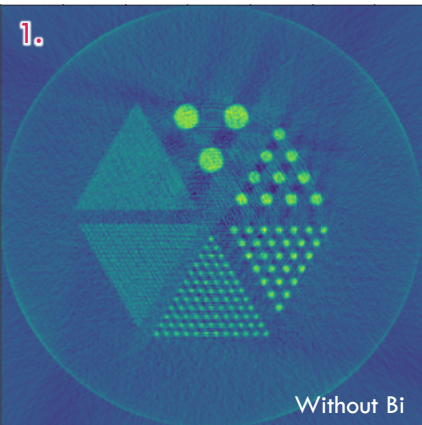
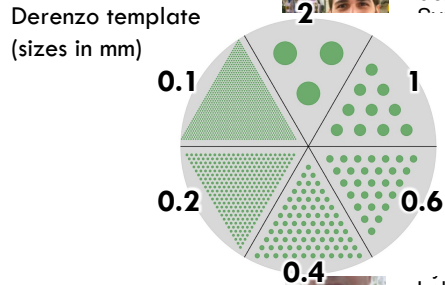


# Performance simulations

## Derenzo phantom for imaging reconstruction

17

- Derenzo phantom to test reconstruction down to given feature size
  - ▣ 2.0, 1.0, 0.6, 0.4, 0.2, 0.1 mm rods (no positron mean free path)
    1. Filtered back projection (FBP)
    2. FBP + sensitivity correction
    3. Iterative TV + sensitivity correction
    4. Iterative TV + sensitivity correction



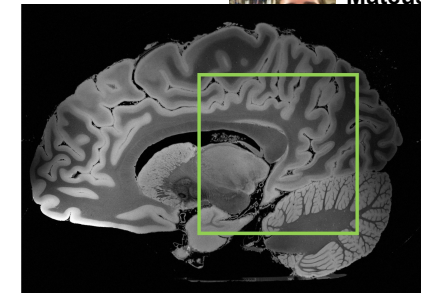
# Performance simulations

## Hi-res MRI/CT image templates

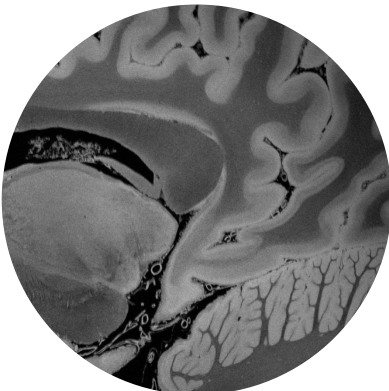
18

Extension of Derenzo template to real medical images

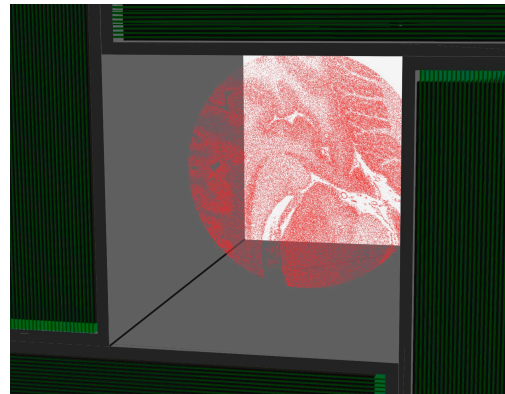
- 7 Tesla MRI of the ex vivo human brain at 100 micron resolution  
[doi:10.18112/openneuro.ds002179.v1.1.0](https://doi.org/10.18112/openneuro.ds002179.v1.1.0)
  - ▣  $68 \times 68 \text{ mm}^2$  ( $680 \times 680$  pixels) resized to  $34 \times 34 \text{ mm}^2$  (scaling pixel resolution to  $50 \times 50 \mu\text{m}^2$ )
  - ▣ Each  $50 \times 50 \mu\text{m}^2$  pixel is used as a plane source, with activity proportional to pixel's grey scale



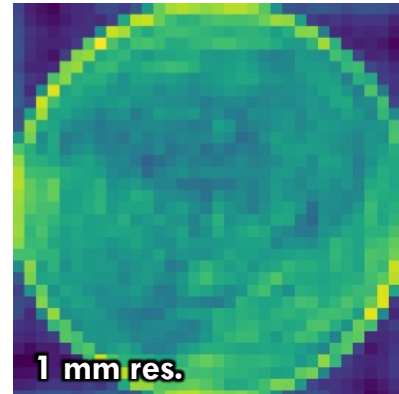
MRI (TIFF) image used



“Image source” placed in the scanner



Reconstruction with typical 1mm res.



# Performance simulations

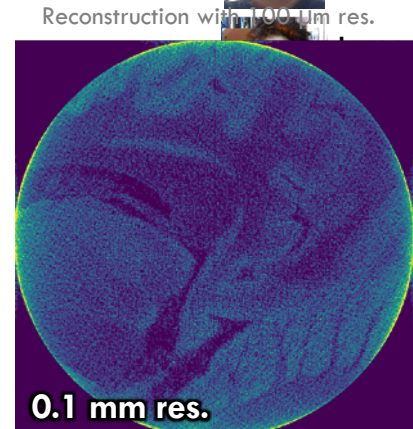
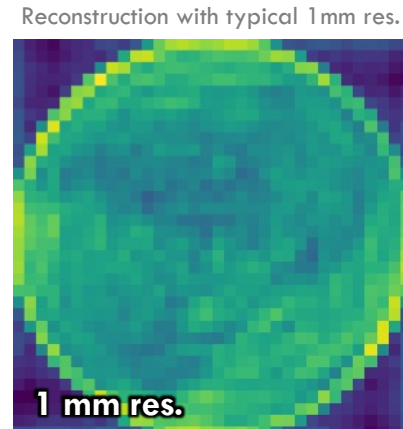
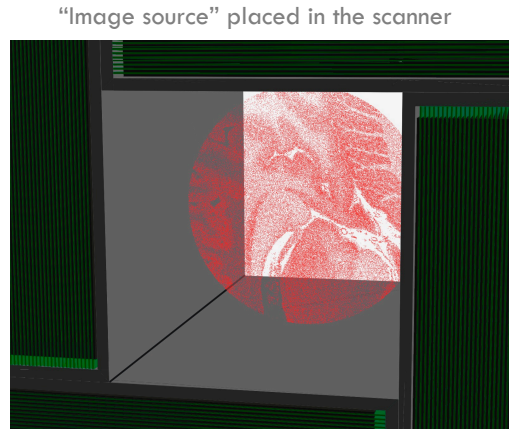
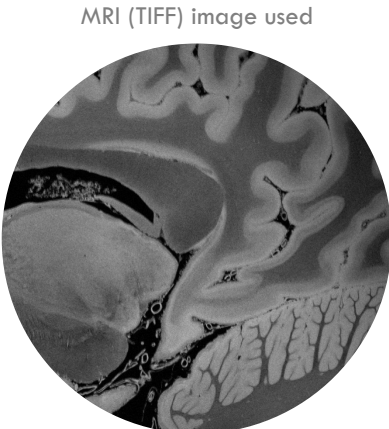
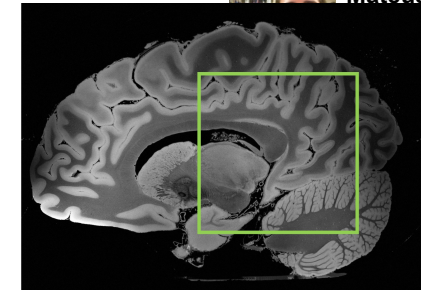
## Hi-res MRI/CT image templates

19

myicente@cern.ch

Extension of Derenzo template to real medical images

- 7 Tesla MRI of the ex vivo human brain at 100 micron resolution  
[doi:10.18112/openneuro.ds002179.v1.1.0](https://doi.org/10.18112/openneuro.ds002179.v1.1.0)
  - ▢  $68 \times 68 \text{ mm}^2$  ( $680 \times 680$  pixels) resized to  $34 \times 34 \text{ mm}^2$  (scaling pixel resolution to  $50 \times 50 \mu\text{m}^2$ )
  - ▢ Each  $50 \times 50 \mu\text{m}^2$  pixel is used as a plane source, with activity proportional to pixel's grey scale
- Results shows that unprecedented details can be reconstructed



# Summary and conclusions

- PET scanners are an important diagnostic tool for metabolic process imaging
  - Continuous improvements over the years (e.g. Time-of-Flight PET with tens of ps; Depth-of-Interaction encoding)
- Potential ultra-high-resolution molecular imaging using **MAPS**
  - ASIC designed within the **UniGE DPNC** group (Together with the FASER and MONOLITH projects)
  - Development of module construction technique based on flip-chip bonding for minimal packaging

# Summary and conclusions

21

- PET scanners are an important diagnostic tool for metabolic process imaging
  - ▣ Continuous improvements over the years (e.g. Time-of-Flight PET with tens of ps; Depth-of-Interaction encoding)
- Potential ultra-high-resolution molecular imaging using MAPS
  - ▣ ASIC designed within the UniGE DPNC group (Together with the FASER and MONOLITH projects)
  - ▣ Development of module construction technique based on flip-chip bonding for minimal packaging
- 4.8% and 3.3% scanner sensitivity (w/ or w/o Bismuth layer)
- 0.13-0.21 mm PSF → 0.006-0.017 mm<sup>3</sup> volumetric resolution
  - ❖ In the wish-list: TOF ≤ 10ps, when delivered by the MONOLITH project
- Delivery of a proof-of-concept scanner for small animals in 2025
  - ▣ With silicon-sensor technology advances, its cost will go down and larger scanners can be envisaged in the near future

